# Extreme Ultraviolet Reflection-Absorption (XUV-RA) Spectroscopy: Probing Dynamics at Surfaces from a Molecular Perspective

Somnath Biswas\*,† and L. Robert Baker\*,‡

†Department of Chemistry, Princeton University, Washington Road, Princeton, NJ 08544 ‡Department of Chemistry and Biochemistry, The Ohio State University, Columbus, OH 43210

#### CONSPECTUS:

Extreme ultraviolet (XUV) light sources based on high harmonic generation are enabling the development of novel spectroscopic methods to help advance the frontiers of ultrafast science and technology. In this account we discuss the development of XUV-RA spectroscopy at near grazing incident reflection geometry and highlight recent applications of this method to study ultrafast electron dynamics at surfaces. Measuring core-to-valence transitions with broadband, femtosecond pulses of XUV light extends the benefits of x-ray absorption spectroscopy to a laboratory tabletop by providing a chemical fingerprint of materials, including the ability to resolve individual elements with sensitivity to oxidation state, spin state, carrier polarity, and coordination geometry. Combining this chemical state sensitivity with femtosecond time resolution provides new insight into the material properties that govern charge carrier dynamics in complex materials. It is well known that surface dynamics differ significantly from equivalent processes in bulk materials, and that charge separation, trapping, transport, and recombination occurring uniquely at surfaces governs the efficiency of numerous technologically relevant processes spanning photocatalysis, photovoltaics, and information storage and processing. Importantly, XUV-RA spectroscopy at near grazing angle is also surface sensitive with a probe depth of ~3 nm, providing a new window into electronic and structural dynamics at surfaces and interfaces. Here we highlight the unique capabilities and recent applications of XUV-RA spectroscopy to study photo-induced surface dynamics in metal oxide semiconductors, including photocatalytic oxides (Fe<sub>2</sub>O<sub>3</sub>, Co<sub>3</sub>O<sub>4</sub> NiO, and CuFeO<sub>2</sub>) as well as photoswitchable magnetic oxide (CoFe<sub>2</sub>O<sub>4</sub>). We first compare the ultrafast electron self-trapping rates via small polaron formation at the surface and bulk of Fe<sub>2</sub>O<sub>3</sub> where we note that the energetics and kinetics of this process differ significantly at the surface. Additionally, we demonstrate the ability to systematically tune this kinetics by molecular functionalization, thereby, providing a route to control carrier transport at surfaces. We also measure the spectral signatures of charge transfer excitons with site specific localization of both electrons and holes in a series of transition metal oxide semiconductors (Fe<sub>2</sub>O<sub>3</sub>, NiO, Co<sub>3</sub>O<sub>4</sub>). The presence of valence band holes probed at the oxygen L<sub>1</sub>-edge confirms a direct relationship between the metal-oxygen bond covalency and water oxidation efficiency. For a mixed metal oxide CuFeO<sub>2</sub> in the layered delafossite structure, XUV-RA reveals that the sub-picosecond hole thermalization from O 2p to Cu 3d states of CuFeO<sub>2</sub> leads to the spatial separation of electrons and holes, resulting in exceptional photocatalytic performance for H<sub>2</sub> evolution and CO<sub>2</sub> reduction of this material. Finally, we provide an example to show the ability of XUV-RA to probe spin state specific dynamics in a

the photo-switchable ferrimagnet, cobalt ferrite (CoFe<sub>2</sub>O<sub>4</sub>). This study provides a detailed understating of ultrafast spin switching in a complex magnetic material with site-specific resolution. In summary, the applications of XUV-RA spectroscopy demonstrated here illustrate the current abilities and future promise of this method to extend molecule-level understanding from well-defined photochemical complexes to complex materials so that charge and spin dynamics at surfaces can be tuned with the precision of molecular photochemistry.

## ■ KEY REFERENCES

- Biswas, S.; Husek, J.; Londo S.; and Baker, L. R. Highly Localized Charge Transfer Excitons in Metal Oxide Semiconductors. Nano Lett., 2018, 18, 1228–1233. Direct observation of photoexcited electrons and holes at the metal M<sub>2,3</sub> and oxygen L<sub>1</sub>-edge, respectively in Fe<sub>2</sub>O<sub>3</sub>, Co<sub>3</sub>O<sub>4</sub>, and NiO. Chemical shifts at the O L<sub>1</sub>-edge enable unambiguous comparison of metal-oxygen (M-O) bond covalency.
- Biswas, S.; Wallentine, S.; Bandaranayake, S.; Baker, L. R. Controlling polaron formation at hematite surfaces by molecular functionalization probed by XUV reflection-absorption spectroscopy. J. Chem. Phys., 2019, 151, 104701.<sup>2</sup> XUV-RA provides a systematic comparison between surface and bulk polaron formation kinetics and energetics in photoexcited hematite. The surface polaron formation rate can be systematically tuned by surface molecular functionalization.
- Husek, J.; Cirri, A.; Biswas, S.; Asthagiri, A.; Baker, L. R. Hole Thermalization Dynamics Facilitate Ultrafast Spatial Charge Separation in CuFeO2 Solar Photocathodes. J. Phys. Chem. C., 2018, 122, 11300-11304. Cathodic photocurrent observed in CuFeO2, is shown to correlate with ultrafast (500 fs) hole thermalization from O 2p to hybridized Cu 3d states, leading to spatial charge separation within the CuFeO2 lattice.
- Londo, S.; Biswas, S.; Husek, J.; Pinchuk, I.V; Newburger, M. J.; Boyadzhiev, A.; Trout, A.H.; McComb D.W.; Kawakami, R.; Baker, L. R. Ultrafast Spin Crossover in a Room-Temperature Ferrimagnet: Element-Specific Spin Dynamics in Photoexcited Cobalt Ferrite. J. Phys. Chem. C., 2020, 124, 11368-11375. A XUV spectroscopy to probe charge and spin dynamics in room temperature ferrimagnet. Inter-valence charge-transfer excites a metal-tometal charge transfer transition, which drives spin crossover within sub-picosecond time scale with an internal quantum efficiency of unity.

### 1. INTRODUCTION

Many energy conversion systems rely on heterogenous catalysis to accomplish at surfaces what nature does using molecular assemblies. 5,6 Directly probing electron dynamics at surfaces with chemical state resolution promises to extend molecular-level understanding from well-defined photochemical complexes to heterogeneous interfaces so that energy conversion devices can eventually be tuned with the precision of molecular photochemistry. The major challenge of studying charge and spin dynamics at surfaces is that surfaces present a heterogeneous and inherently complex electronic structure due to under-coordination, 7 interface bonding, 8 and chemical and structural defects. 6 Additionally, it is well established that the bulk electronic properties and photophysical dynamics of materials are significantly different from the analogous dynamics occurring at surfaces. 9,10 As a result, photo-physical reaction dynamics at solid surfaces are not very well understood.

Obtaining a molecular understanding of these processes is difficult due to the challenge of probing surfaces with ultrafast time resolution as well as the required chemical state sensitivity to observe the transient evolution of oxidation state, spin state, lattice distortions, electron-phonon coupling and carrier thermalization on individual elements. In time resolved spectroscopy of molecular systems, spectral signatures are directly correlated with coupling between electronic and vibrational excitations, which control important processes such as charge migration, 11,12 intra and intermolecular vibrational relaxation, <sup>13</sup> internal conversion, <sup>14</sup> and intersystem crossing. 15 Translating these processes to dynamics at surfaces, semiconductor photochemistry similarly depends on the kinetics of interfacial charge transport, hot carrier cooling, trapping, and recombination. These processes represent the solid-state analog of excited state relaxation dynamics in molecules. However, the challenge of probing these pathways and their associated rates with ultrafast time resolution and surface sensitivity motivates the goal to extend a molecular-level understanding to dynamics at surfaces and interfaces. In this article, we describe recent progress toward this goal uniquely enabled by XUV-RA spectroscopy, which provides the ability to observe dynamics at surfaces by probing state-specific, core-to-valence transitions with surface sensitivity and ultrafast time resolution.

This progress is facilitated by the ability to produce ultrafast, broadband pulses of XUV light by tabletop high harmonic generation (HHG). <sup>16</sup> Using ultrafast XUV light produced by HHG, it is possible to perform absorption measurements similar to x-ray absorption spectroscopy. <sup>17,18</sup> In x-ray absorption the absolute core-to-valence transition energy serves as an element specific tag similar to x-ray photoelectron spectroscopy, while the absorption lineshape can be interpreted as a projection of the valence band electronic structure. Although this picture of a single electron excitation is a useful approximation, multi-electron interactions may also influence the measured systems and should be considered.

To accurately calculate absorption cross sections, it is necessary to know the true initial and final state wavefunctions. An alternative to these challenging, multibody calculations is the one electron approximation. In this approximation, the initial state is a core wave function, the final state is a free electron wave function, and all the other electrons are considered to not participate in the transition. Within this approximation the absorption spectrum resembles the

partial density of empty states projected onto the core orbital of the absorbing site. Although this approximation can accurately describe K-edge transitions (1s  $\rightarrow$  4p) for the 3d transition metals, it often breaks down for L-edge (2p  $\rightarrow$  3d) and M-edge (3p  $\rightarrow$  3d) transitions, where the interaction of the core-hole with the 3d valence band is significant. These interactions can be partially accounted for by considering angular momentum coupling between the core-hole and the partially filled valence band, and this treatment is the basis for ligand field multiplet simulations of x-ray absorption spectra.  $^{17,19}$  X-ray absorption spectroscopy has been widely used to measure local coordination and electronic structure with element-specific resolution in a variety of molecular systems.  $^{20,21}$ 

As XUV light also probes core-to-valence transitions, XUV absorption spectroscopy based on HHG offers the benefits of performing x-ray absorption spectroscopy on a laboratory tabletop, providing element-specific resolution with sensitivity to oxidation state, spin state, carrier polarity, and coordination geometry. <sup>4,18,22,23</sup> This means that in ultrafast XUV measurements it is possible to resolve the contribution of individual atoms to the overall charge and spin dynamics of a material. In this way XUV spectroscopy fills an important gap by combining the time resolution inherent in ultrafast optical methods with the chemical state resolution typical of x-ray absorption methods. <sup>24</sup>

To extend this method to the study of surface dynamics, we have recently pioneered a reflection analog to XUV transient absorption and demonstrated that measuring XUV reflectance at near grazing angle represents a surface specific measurement with a sampling depth  $\leq 3$  nm. <sup>25</sup> As described in this article, this method is now enabling real time observation of dynamics at surfaces with the ability to resolve element, <sup>26</sup> oxidation state, <sup>27</sup> spin state, <sup>4,28</sup> coordination environment, <sup>4</sup> and carrier specific <sup>1</sup> dynamics with femtosecond time resolution. The examples provided highlight the ability of this method to address the long-standing challenge of obtaining a molecule-level understanding of surface dynamics in complex materials.

### 2. ADVANTAGES OF XUV SPECTROSCOPY

## 2.1 Resolving Oxidation State, Spin State and Coordination Geometry with Element Specificity

In this section, we describe how XUV spectroscopy based on HHG extends the benefits of x-ray absorption spectroscopy to a tabletop laboratory instrument. 16,30 HHG is an highly nonlinear, strong field process that operates in the nonpurterbative regime. It enables production of XUV and soft x-ray pulses with femtosecond to attosecond pulse durations. The maximum photon energy produced during HHG is proportional to the electron pondermotive energy  $(U_p)$  gained in the strong laser field plus the ionization potential of the generation medium ( $I_p = 24.6$  eV for helium). The pondermotive energy scales with  $\lambda^2$  of the driving laser, where longer wavelengths give rise to greater electron acceleration resulting in higher photon energies. 16 By this process 800 nm pulses can produce XUV photon energies >100 eV, and longer wavelength driving fields can extend the HHG spectrum into the soft x-ray region (>300 eV). Our study focuses on the M<sub>2,3</sub>-edges of the first row transition metals that range from 30 to 80 eV. This range of photon energy is readily accessed using the 800 nm output of a Ti:Sapphire chirped pulse amplifier. A schematic diagram of tabletop

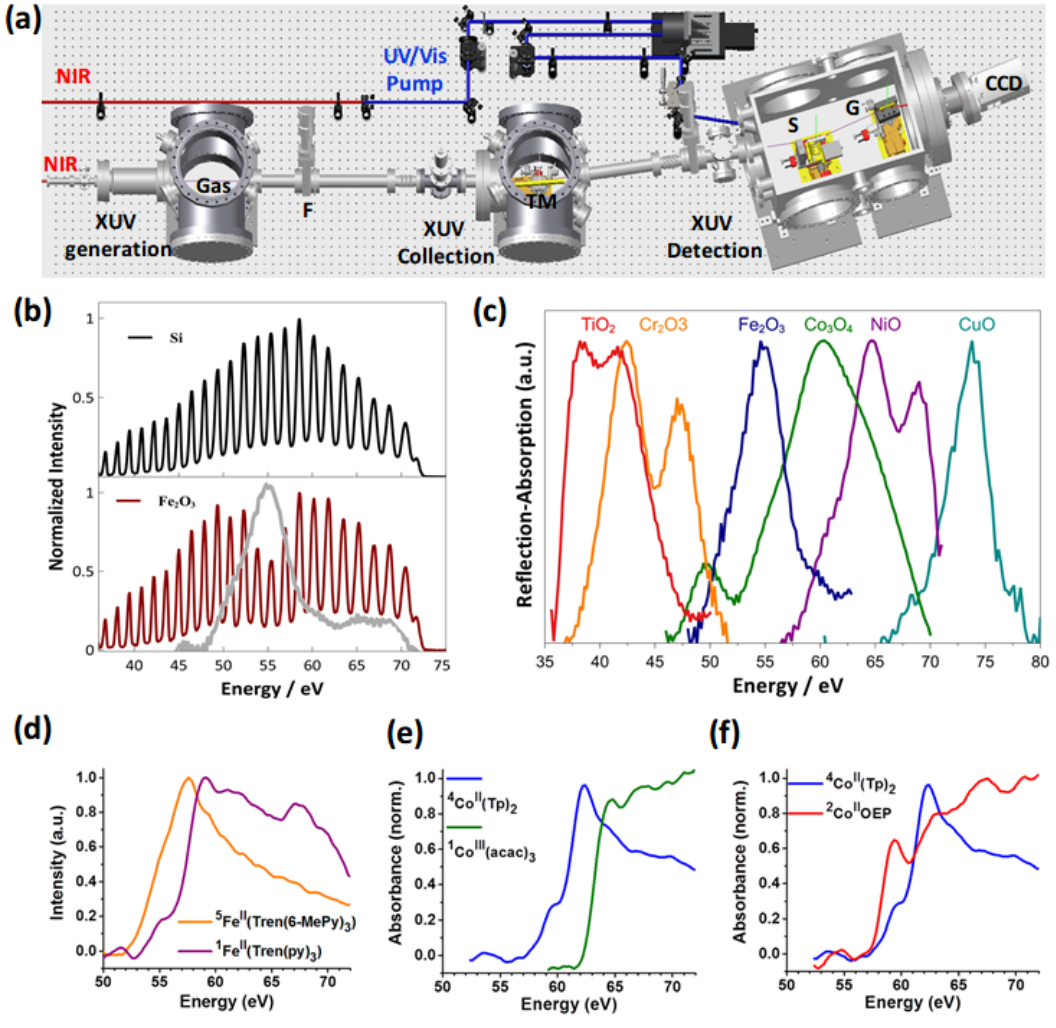


Figure 1. (a) Schematic of XUV-RA spectrometer (b) The high harmonics of He reflected from the Si and  $Fe_2O_3$  substrate. The gray lineshape shows the XUV-RA of  $Fe_2O_3$  (c) XUV-RA line shapes for a series of first row transition metal oxides, showing the element specificity of XUV spectroscopy. (d) spin (e) oxidation state (f) and geometric environment specificity of XUV-RA spectroscopy. Panel a is adapted with permission from ref. 27. Royal Society of Chemistry. Panel c is reproduced with permission from ref. 29. Copyright 2020 American Chemical Society. Panel d, e, f are reproduced with permission from ref. 22. Copyright 2016 American Chemical Society.

XUV spectrometer in a reflection geometry is provided in Figure 1a. 27 In this setup, broadband high harmonics (Figure 1b) are generated in helium via a two-color driving field  $(2mJ \text{ of } 800nm \text{ and } 40\mu J \text{ of } 400nm)$ . Here the 400 nm pulse serves to break to symmetry of the 800 nm field to allow production of both even and odd harmonics. These fundamental beams are filtered using an Al foil (F), which transmits the XUV beam. A toroidal mirror (TM) is used to focus the XUV beam on the sample (S) at a near grazing incidence (8°). A spherical variable line-spaced grating (G) is used to spectrally disperse the XUV beam on to a CCD detector. The broadband high-harmonics reflected off a silicon substrate extend from 30-72 eV, as shown in Figure 1b, where the cutoff at 72 eV is defined by the transmission of the Al filter. If a specific core-to-valence absorption edge falls within this energy range, this light-source has the advantage of measuring element, oxidation state, spin state, and geometric environment specific information similar to traditional x-ray absorption edges.

To show the capability of element specificity of XUV spectroscopy, Figure 1c compares the XUV absorption lineshapes for a series of first row transition metal oxides in a reflection geometry.  $^{25,29}$  The absorption lineshapes are a result

of  $M_{2,3}$ -edge absorption which corresponds to the  $3p \rightarrow 3d$ transitions. The  $M_{2,3}$ -edge transition energy increases with the atomic number as the effective nuclear charge increases from left to right of the periodic table, retaining the element specific signature of core-to-valence spectroscopy. Measurements by Zhang et al. on bulk molecular thin film systems show that the shape and position of these absorption edges are additionally sensitive to the spin state (Figure 1d), oxidation state (Figure 1e), and coordination geometry (Figure 1f) of the respective metal center. <sup>22</sup> XUV-RA measurements of ferrimagnetic spinel metal oxides also demonstrate the sensitivity of this method to spin state, oxidation state, and coordination geometry. 4,28 It should be noted that the advantages of XUV spectroscopy described in this section are general phenomena of core-level spectroscopy ranging from XUV spectral domain to soft and hard x-ray regime. However, the ability to measure core-hole spectra using a tabletop instrument with ultrafast time resolution combined with the surface specificity of XUV light make XUV-RA spectroscopy uniquely suited to provide a detailed understanding of dynamics at surfaces.

#### 2.2 Surface Specificity

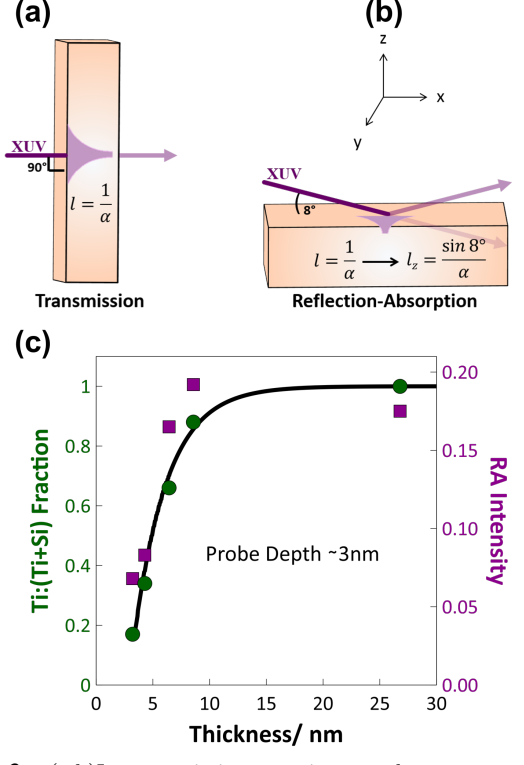


Figure 2. (a,b)In transmission experiments, the resonant attenuation of the transmitted beam is inversely proportional to the attenuation coefficient  $\alpha$ . For grazing angle reflection geometry the depth of interaction decreases by a factor of  $sin\theta$ . (c) The experimentally determined probe depth for XUV-RA spectroscopy and XPS. Fitting an exponential rise to the XPS data points yields a probe depth of 2.8 nm (shown by the black line). Reproduced with permission from ref. 26. Copyright 2018 Royal Society of Chemistry

As described above, the difficulty of making chemically precise, state-resolved measurements of surface dynamics represents a significant challenge. 31–34 Many theoretical studies predict that equilibrium structure as well as non-equilibrium dynamics of charge carriers at surfaces are very different compared to the equivalent processes in bulk. 35–37 This can be a result of undercoordination of surface atoms, interface bonding, and surface segregation of structural defects, all which can be difficult to accurately characterize. 6–8,33 Accordingly, correct understanding of charge and spin dynamics at surfaces, which are relevant for numerous processes in energy conversion and information processing, require the ability to make state-resolved surface sensitive measurements with ultrafast time resolution.

To address this challenge, we designed a time-resolved XUV spectrometer in a reflection geometry, where the XUV probe beam reflects from a sample surface at a near grazing incidence angle. <sup>25</sup> Figure 2a and b qualitatively show the advantage of performing a reflection experiment compared to a transmission measurement in terms of the attenuation length, which defines the probe depth. Compared to a transmission geometry, the attenuation length of XUV light projected along the surface normal at near grazing incidence is reduced by a factor of  $\sin(\theta)$ , where  $\theta$  is the incidence angle of the probe beam relative to the sample plane. <sup>26</sup> In this present experimental design, near grazing angle is set to 8°, reducing the probe depth by a factor of 7.2 . For a series of first row transition metal oxides, this limits the interaction

of the probe beam in these reflection measurements only a few nm from the sample surface (Table 1), enabling surface sensitive measurements. Although this report is focused primarily on the first row transition metal oxides, the resonant attenuation length of XUV light is similarly low for many materials, <sup>38</sup> indicating this technique can be applied more generally to probe surface dynamics in a wide range of material systems. XUV spectroscopy in a reflection geometry can also be used measure complex dielectric functions in the XUV region <sup>39</sup> and is sensitive to changes in the non-resonant photo-ionization cross-section of materials. <sup>40</sup>

It should be noted that line shapes differ for reflection spectra compared to absorption spectra because absorption depends only the imaginary component of the refractive index, while reflection depends on the complex refractive index. However, because real and imaginary components of the complex index represent Kramers-Kronig pairs, the same resonance information is inherently contained in either measurement. In fact, we have shown that absorption simulations can also predict reflection spectra, under the assumptions required for Kramers-Kronig transformations. Interested readers are referred to previous work <sup>25,27</sup> for details of interpreting XUV-RA lineshapes using semi-empirical charge transfer multiplet theory and classical electromagnetic theory.

**Table 1.** Attenuation coefficients and probe beam interaction regions in transmission and reflection-absorption experiments for  $\text{Fe}_2\text{O}_3$ ,  $\text{Co}_3\text{O}_4$ , and NiO. Adapted from Ref. 26 with permission from the Royal Society of Chemistry

Metal oxide	$lpha \ / \ \mathrm{nm}^{-1}$	$l_z$ / nm
Fe <sub>2</sub> O <sub>3</sub>	$0.102^{18}$	1.36
$Co_3O_4$	$0.036^{41}$	3.87
NiÖ	$0.064^{38}$	2.17
$TiO_2$	$0.136^{38}$	1.02

In order to experimentally validate the predicted surface specificity of XUV-RA, we compare the probe depth of XUV-RA with a widely used surface analysis technique, x-ray photoelectron spectroscopy (XPS). It is expected that for XUV-RA measurements as a function of film thickness, the measured XUV-RA intensity should saturate beyond the limit where the material thickness exceeds the probe depth. <sup>38</sup> To verify this, we plot the XUV M<sub>2,3</sub>-edge resonant intensity of  $TiO_2$  films grown by atomic layer deposition on a  $SiO_2$ substrate as a function of TiO<sub>2</sub> film thickness (Figure 2c). <sup>25</sup> As expected, we observe an intensity saturation at higher film thickness, and the probe depth is defined by fitting this curve to an exponential. For comparison, the probe depth of XPS is obtained from the same samples by measuring the atomic fraction of Ti as a function of film thickness, and this result obtained by XPS follows nearly identical fit (Figure 2c). 25 The best fit to these data provides a measured probe depth of 2.8 nm, confirming that XUV-RA is well-suited to elucidate ultrafast dynamics at surfaces with chemical state resolution. It has also been shown that XUV-RA is sensitive to photoemission cross sections through the nonresonant offset of the imaginary refractive index. 40

Utilizing the surface specificity, we compare the time-resolved surface and bulk polaron formation dynamics in hematite, an earth abundant photocatalyst, which suffers from poor carrier mobility due to small polarons. 40,42–44 In the photoexcited state of hematite, the excited electrons couple to optical phonons, resulting in an ultrafast lattice distortion and small polaron formation within several hundred femtoseconds. This process severely limits charge carrier

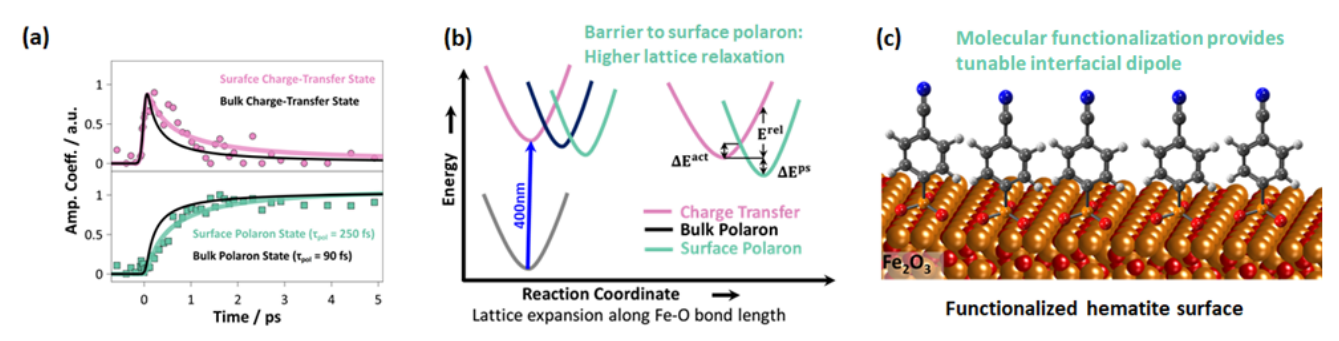


Figure 3. (a) Comparing surface vs bulk polaron formation rates. Amplitude coefficients calculated from experimental data are shown in pink circles (charge-transfer state) and cyan squares (polaron state) and the fits to the coefficients are represented by solid lines. Black solid line represents the corresponding fits for bulk measurements. (b) Marcus model for electron transfer along the Fe-O reaction coordinate. Marcus parameters required to describe this process include the activation energy ( $\Delta E^{act}$ ), relaxation energy ( $E^{rel}$ ), and polaron stabilization energy ( $E^{rel}$ ). (c) Schematic representation of functionalized hematite surfaces. Reproduced with permission from ref. 2. Copyright 2019 AIP Publishing.

mobility and increases recombination events. For Fe<sub>2</sub>O<sub>3</sub> it has been predicted that the kinetics of polaron formation and hopping are unique to the surface, but converge to bulk values within 3-4 atomic layers. <sup>45</sup> Using XUV-RA we measure these surface kinetics, which confirm that the polaron formation time constant ( $\tau_{pol} = 250 \pm 40$  fs) is about three times slower compared to bulk (90 ± 5 fs) as shown in Figure 3a. <sup>42</sup>

To understand this significant difference, we consider a Marcus polaron hopping model as illustrated in Figure 3b and described in Equation 1. The parabolas in this Marcus model represent the potential energy surfaces of the same states observed in XUV measurements, where the initial excited state is the charge transfer state, and the self-trapped or stabilized state is the small polaron. Here the reaction coordinate primarily represents expansion of the Fe-O bond at photoexcited  ${\rm Fe}^{2+}$  centers.

$$\Delta E^{act} = \frac{(\Delta E^{ps} + E^{rel})^2}{4E^{rel}} \tag{1}$$

In Equation 1,  $\Delta E^{ps}$  is the polaron stabilization energy, which can also be described as the thermodynamic driving force of polaron formation, and  $E^{rel}$  is the lattice reorganization energy associated with polaron formation.  $^{46,47}$ From the measured rate we calculate the activation barrier of polaron formation (239  $\pm$  8 meV), which is about 50 meV greater than in bulk. Analysis shows that this difference is a result of lower steric hindrance at the surface, accommodating greater lattice reorganization  $(E^{rel})$  along the Fe-O reaction coordinate. We also show this barrier is tunable based on surface functionalization with organic molecules (Figure 3c), which can stabilize or destabilize the surface polaron state by controlling the interfacial dipole moment. This study demonstrates the use of XUV-RA spectroscopy to probe time-resolved dynamics at surfaces, and provides a new direction for improving interfacial charge transport at hematite surfaces based on molecular understanding the electron trapping process.

## 3. CARRIER SPECIFICITY OF XUV SPECTROSCOPY

Probing photoexcited dynamics with carrier specificity refers to the ability to independently resolve charge carriers with opposite polarity (i.e. electrons vs holes). Although challenging, this ability has the potential to provide unique chemical insights into the ultrafast processes that ultimately determine charge separation and transport in complex materials. <sup>49</sup> Optical spectroscopy in the visible and ultra-violet regime probes the joint density of states, therefore separating the signatures of electrons and holes in the frequency space is difficult. 48 Consequently, time-resolved observation of electron and hole thermalization simultaneously in the optical regime is challenging due to the overlapping spectral features of electrons and holes. Because XUV probes core transitions, separate signature of electrons and holes can be obtained through transitions from core orbitals to conduction and valence bands, respectively. We note that hard xray spectroscopy has also been used to probe the dynamics of both electrons and holes in metal oxides and inorganic perovskites materials. 50-52 Here we provide several illustrative examples where tabletop XUV spectroscopy has been used to independently resolve the signature of both electrons and holes simultaneously.

Figure 4a shows a simple molecular orbital diagram of a M-O bond where photoexcitation produces electrons in the metal based 3d orbitals and holes in the hybridized M (3d) and O (2p) orbitals. 1 According to this diagram, the metal M<sub>2,3</sub>-edge absorption informs the electron dynamics where the O L<sub>1</sub>-edge absorption enables detection of photo excited hole dynamics. Figure 4b compares the transient XUV-RA spectra after 2 ps following photoexcitation for Fe<sub>2</sub>O<sub>3</sub>, Co<sub>3</sub>O<sub>4</sub>, NiO and FeS<sub>2</sub>. In each case the shaded background represents the static XUV-RA spectrum to the corresponding transient spectrum. Photoexcited states in Fe<sub>2</sub>O<sub>3</sub>, Co<sub>3</sub>O<sub>4</sub> and NiO each show a similar nature of the charge transfer excited states where photoexcitation (O 2p→M 3d) leads to one-electron reduction of the respective metal centers. In addition to the spectral features corresponding to the metal M<sub>2,3</sub>-edge transitions of Fe, Co, and Ni, which increase from 50 to 70 eV, we observe an additional excited state absorption feature around 42 eV, which appears consistently in Fe<sub>2</sub>O<sub>3</sub>, Co<sub>3</sub>O<sub>4</sub> and NiO as shown in Figure 4b. According to the Henke table, this common positive absorption feature observed at 42 eV matches the O L<sub>1</sub>-edge (2s $\rightarrow$ 2p) transition energy (41.6 eV) and is assigned to the hole in the O 2p based valence band following photoexcitation as schematically depicted in Figure 4a. <sup>38</sup> The spectral feature in FeS<sub>2</sub> at the Fe M<sub>2,3</sub>-edge is similar to Fe<sub>2</sub>O<sub>3</sub>, however, no positive feature around 42 eV is observed in FeS<sub>2</sub>. This observation confirms that the positive feature at 42 eV represents the O L<sub>1</sub>-edge transition associated with the presence of a transient hole in the O 2p based valence band in pho-

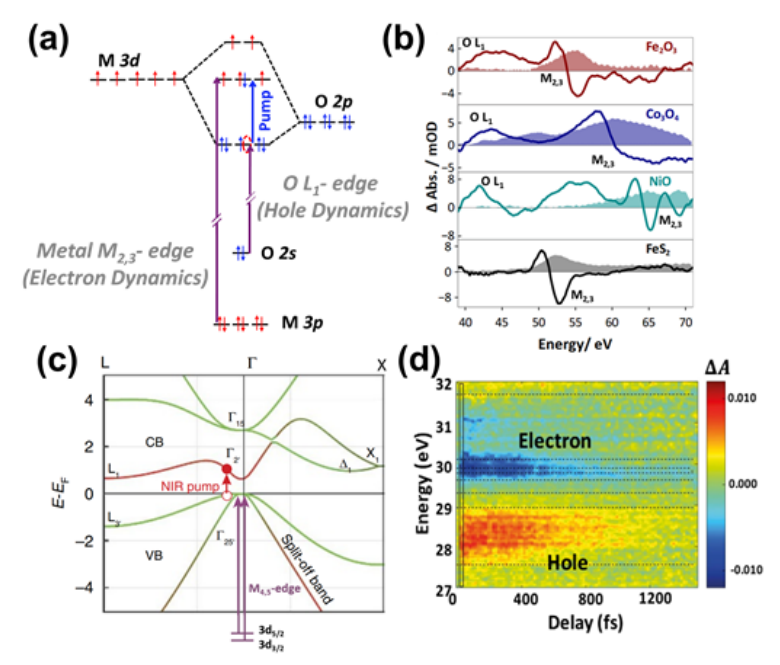


Figure 4. (a) A simplified molecular orbital picture of M-O bond. O  $L_1$ -edge absorption is enabled after photoexcitation which removes an electron from the filled 2p shell (b) Transient XUV-RA spectra of  $Fe_2O_3$ ,  $Co_3O_4$ , NiO, and  $FeS_2$  after 2 ps following photoexcitation. Shaded plots represent the corresponding measured static XUV-RA spectra. Both metal  $M_{2,3}$ -edge and O  $L_1$ -edge absorption are identified. (c) Band diagram for germanium, showing that the VIS-NIR pump pulse initially promotes electrons (filled red circle) into the CB leaving behind holes (open red circle) in the VB. XUV  $M_{4,5}$ -edge absorption can probe the electrons and holes simultaneously. (d) Carrier dynamics in nanocrystalline germanium reveal the independent signature of photoexcited holes in the valence band (VB) and electrons in the conduction band (CB). Panel a and b are adapted with permission from ref. Copyright 2018 American Chemical Society. Panel c and d are adapted with permission from ref. 48 Copyright 2017 Nature Publishing Group.

to excited  $\rm Fe_2O_3,~Co_3O_4$  and NiO. The localization of the hole in O 2p valence band and the electron in the M 3d conduction band confirms the nature of the charge-transfer exciton in this series of metal oxide semiconductors.

Additionally, the spectral feature at the O  $L_1$ -edge in each metal oxide shows that there is a gradual red-shift of the  $L_1$ edge peak position from Fe<sub>2</sub>O<sub>3</sub> to Co<sub>3</sub>O<sub>4</sub> to NiO. This trend is associated with the M-O bond covalency in these metal oxides. To explain, as M-O bond covalency increases, the O 2p bonding states are stabilized. This shift of the O 2p states decreases the O L<sub>1</sub> transition energy occurring from the O 2s core to the O 2p valence band. Therefore, transient XUV spectroscopy is directly probing the M-O bond covalency in these metal oxides in the photoexcited state by sampling the stabilization of the valence band hole. Ground state O K-edge x-ray absorption can indirectly probe the M-O bond covalency because it represents a measure of the O 2p character in the unoccupied metal 3d conduction band states. However, accurate interpretation of M-O bond covalency requires knowledge of the metal 3d occupancy as well as the relative hybridization of O 2p states with the metal  $e_q$  and  $t_{2q}$  conduction band states, making a comparison of covalency difficult, particularly for the late transition metal oxides. 53

Metal oxides are a compound semiconductor with different elemental contributions to the electron and hole wavefunctions, but XUV can also differentiate carriers in single element semiconductors. For example, XUV transient absorption spectroscopy of Ge and Si reveals spectrally resolved signatures of electrons and holes, and their time-resolved dynamics can be independently measured as shown in Figure 4c and d.  $^{48,54,55}$  In a related experiment on  $\mathrm{Si}_{0.25}\mathrm{Ge}_{0.75}$  alloy, it was possible to detect electron trapping to detect

states near the conduction bands by probing Ge M4, 5 absorption.  $^{56}$  Similarly, Lin *et. al.* observed separate signatures of electrons and holes by probing the I 4d core level (I N<sub>4,5</sub>-edge) transitions in photoexcited PbI<sub>2</sub>.  $^{23}$  Recently, Attar et al. observed carrier specific relaxation in nanoscale thin films of layered 2H-MoTe<sub>2</sub> semiconductor.  $^{57}$ 

## 4. ULTRAFAST SPATIAL CHARGE SEPARATION IN CuFeO<sub>2</sub> SOLAR PHOTOCATHODES

CuFeO<sub>2</sub> is an earth-abundant metal oxide semiconductor, showing promising ability as a solar photocathode for  $\rm H_2$  evolution and  $\rm CO_2$  reduction.  $^{58,59}$  Analogous to Fe<sub>2</sub>O<sub>3</sub>, photoexcitation of CuFeO<sub>2</sub> excites electrons from O 2p valence band to Fe 3d conduction bands, however, cathodic photo current is only observed in  $CuFeO_2$  as shown in Figure 5a. A clear mechanism for the exceptional photocatalytic performance of CuFeO<sub>2</sub> is not well understood. With the ability of XUV-RA spectroscopy to observe element, oxidation state, and carrier specific dynamics, we find that a subpicosecond spatial separation of photoexcited electrons and hole occurs within the CuFeO<sub>2</sub> delafossite lattice. In particularly, hole thermalization from O 2p to Cu 3d states of CuFeO<sub>2</sub> leads to the spatial separation of electrons and holes which cannot occur in Fe<sub>2</sub>O<sub>3</sub>. This spatial charge separation in CuFeO<sub>2</sub> is enabled by the layered delafossite structure, where interband hole thermalization results in spatial separation of holes from electrons across separate layers of this material.<sup>3</sup>

Figure 5b and c compare the XUV-RA spectra of photoexcited  $Fe_2O_3$  and  $CuFeO_2$ , respectively as a function of time. The spectral features of  $Fe_2O_3$  at the Fe  $M_{2,3}$ -edge (50-60 eV) consist of a ground state bleach at 54 eV which is associated with the charge transfer state. This bleach feature

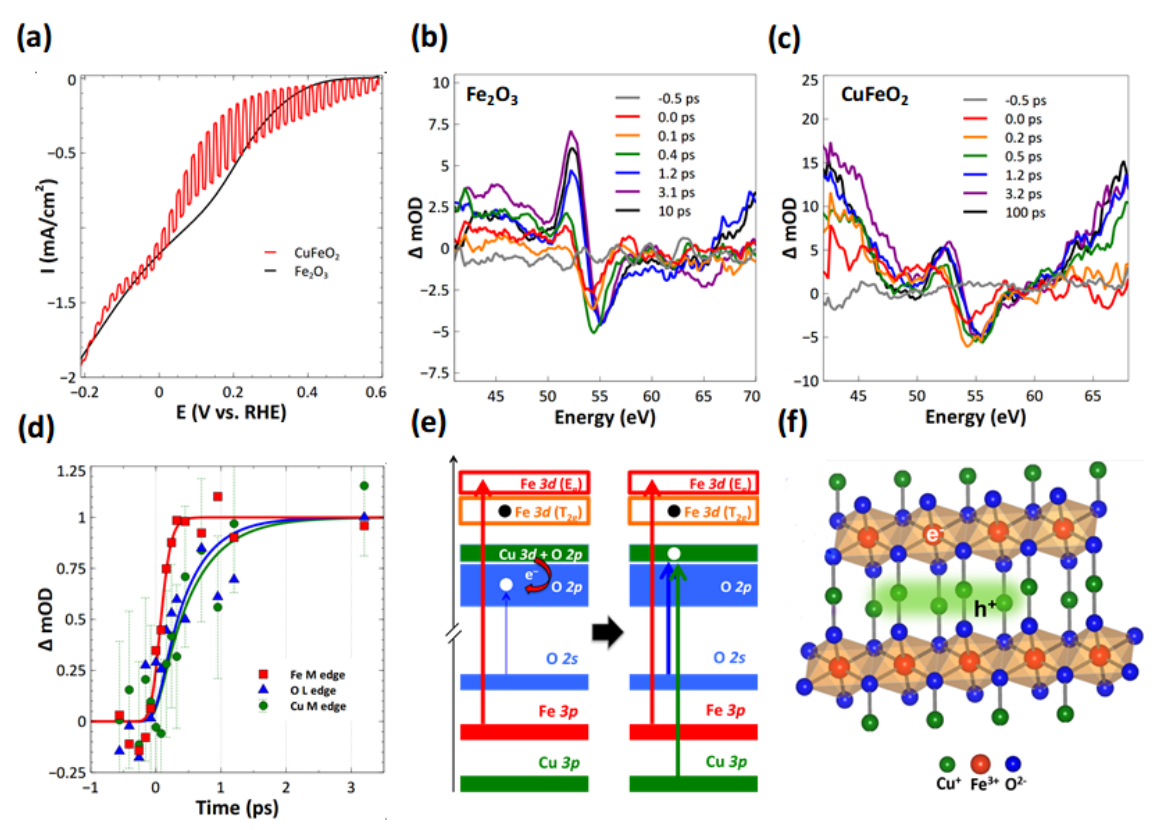


Figure 5. (a)Linear sweep voltammograms for  $CuFeO_2$  (red) and  $Fe_2O_3$  (black) during illumination with a chopped light source. For the case of  $Fe_2O_3$  no photoinduced cathodic current is observed. By comparison, delafossite  $CuFeO_2$  displays significant catalytic photocurrent. Transient XUV-RA spectra of (b)  $Fe_2O_3$  and (c)  $CuFeO_2$  as a function of time. (d) Normalized kinetic traces showing the transient response at the Fe  $M_{2,3}$ -edge, the  $CuM_{2,3}$ -edge, and the  $OL_1$ -edge. (e) Schematic showing the time evolution of XUV transient reflectionabsorption features for an initial  $O2p \rightarrow Fe$  3d charge transfer excitation followed by hole thermalization to strongly hybridized Cu 3d states at the valence band edge. (f) Spatial separation of electrons and holes within the  $CuFeO_2$  lattice, where electrons localizes to the Fe 3d centers and holes localizes to the Cu 3d centers in between the layers of Fe octahedra. Adapted with permission from ref. 3. Copyright 2018 American Chemical Society.

blue-shifts as a function of time with a correlated formation of excited state absorption at 52 eV within few hundreds of femtoseconds. This is a signature of lattice expansion associated with surface electron trapping and small polaron formation. 27 Similar kinetics and spectral features were observed in case of photoexcited CuFeO<sub>2</sub> at the Fe M<sub>2,3</sub>-edge (50-60 eV), indicating the presence of similar charge transfer state and surface electron trapping dynamics. However, in case of CuFeO<sub>2</sub>, interestingly we observe strong excited state absorption at the O L<sub>1</sub>-edge (40-47 eV) and Cu  $M_{2,3}$ -edge (above 63 eV). Time evolution of these features is correlated in time (Figure 5d) and delayed (time constant of  $\sim 500 \text{fs}$ ) with respect to the near-instantaneous transient signal observed at the Fe  $M_{2,3}$  edge. These observations are explained schematically in Figure 5e. Photoexcitation creates a charge transfer state where transient holes are localized in O 2p valence bands, while the electrons are localised in Fe 3d conduction bands. However, at a measurable, sub-picosecond time delay following photoexcitation, the hole thermalization occurs from the O 2p valence bands to the hybridised Cu 3d and O 2p orbitals near the valence band maximum. As the hole thermalizes to these hybridised Cu 3d and O 2p valence bands, two additional channels of XUV transitions appear 1) O 2s $\rightarrow$  Cu 3d + O 2p (O L<sub>1</sub>) 2) Cu 3p $\rightarrow$  Cu 3d + O 2p (Cu  $M_{2,3}$ ). We note that although the electron localizes in the Fe 3d conduction band states in both Fe<sub>2</sub>O<sub>3</sub> and CuFeO<sub>2</sub>, hole thermalization in CuFeO<sub>2</sub> facilitates the

sub-picosecond spatial separation of charge carriers (Figure 5f). Therefore, ultrafast hole thermalization in  ${\rm CuFeO_2}$  from localized O 2p to the delocalized hybridized O 2p and Cu 3d valence bands weakens the exciton binding energy and is likely responsible for the significantly improved photocatalytic performance. These results are supported by DFT calculations confirming strong covalency of Cu 3d and O 2p states at the valence band through pCOHP calculations.

These findings are also consistent with x-ray absorption and resonant inelastic x-ray scattering measurements of CuFeO<sub>2</sub>, which have assigned photoexcitation in this material to a metal-to-metal (Cu<sup>+</sup>/Fe<sup>3+</sup>  $\rightarrow$  Cu <sup>2+</sup>/Fe<sup>2+</sup>) charge transfer leading to hole localization in Cu 3d valence band states and electron localization to the Fe 3d conduction band. <sup>60</sup> However, the XUV measurements described here benefit from a 3 order of magnitude increase in time resolution (<100 fs for tabletop XUV spectroscopy compared to 100 ps for third generation synchrotrons), so synchrotron-based measurements are unable to see the ligand-to-metal charge transfer character in the initial photoexcited state or the sub-picosecond spatial charge separation leading to the final metal-to-metal charge transfer state.

## 5. ULTRAFAST SPIN SENSITIVE DYNAMICS

Another important application for XUV-RA spectroscopy is to probe time-resolved spin sate specific dynamics. Here we show an example of this capability using cobalt ferrite

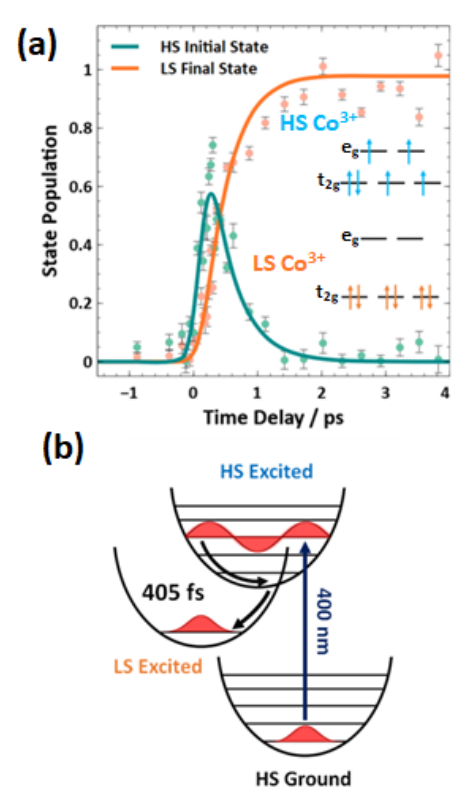


**Figure 6.** (a) Global analysis of SCO dynamics in  $CoFe_2O_4$  from HS initial state to LS final state (b) Depiction of ultrafast intersystem crossing in photoexcited  $CoFe_2O_4$ . Adapted with permission from ref. 4. Copyright 2020 American Chemical Society.

(CFO) as a model system. CFO is a metal oxide semiconductor that belongs to the class of ferrimagnetic inverse spinel ferrites having the general formula CoFe<sub>2</sub>O<sub>4</sub> where, Fe<sup>3+</sup> occupies all of the tetrahedral sites and half of the octahedral sites, and Co<sup>2+</sup> occupies the remaining half of the octahedral sites. In this material all the metal centers are in the high-spin state with the tetrahedral and octahedral sublattices aligned antiparallel to each other to create ferrimagnetic ordering with a nonvanishing magnetization. Interestingly, CFO has a similar valence shell structure comparable to Co-Fe prussian blue analogues (PBAs), therefore there exists the possibility of photoinduced spin crossover via charge-transfer induced spin transition (CTIST). XUV RA measurements confirm this, showing that excitation with 400 nm light leads to a high spin (HS) to low spin (LS) transition on photoexcited Co<sup>3+</sup> with near unity internal quantum efficiency. The kinetic data in Figure 6a represents amplitude coefficients for an initial and final state obtained by global kinetic analysis of the experimental data. Using ligand field multiplet simulations, the initial state (blue) is assigned as a HS Co<sup>3+</sup>, and the final state (orange) is assigned as a LS Co<sup>3+</sup> state. <sup>4</sup> Based on this kinetic analysis we find that the time constant for photo-induced spin crossover (SCO) is  $405 \pm 29$  fs. This sub-picosecond time constant for SCO is similar to the case for several PBAs reported before. Therefore, CFO thin films are able to show CTIST following photo excitation with a 400nm light that drives the system to a MMCT state where Co<sup>3+</sup> is initially in a HS state, which subsequently relaxes to a LS  $Co^{3+}$  state within few hundreds of femtoseconds (Figure 6b). In a related study on nickel ferrite, we similarly observed optical spin state switching with element specific resolution. 2

### 6. SUMMARY AND FUTURE DIRECTIONS

XUV-RA spectroscopy is currently extending a molecular-level understanding of dynamics at surfaces from well-defined photochemical complexes to complex material interfaces. An important emerging direction is to extend HHG to the water window (280-535 eV) and utilize these light sources to access C, N and O K-edges to study dynamics of solvated systems in liquid environments. A number of studies have demonstrated spectroscopy at the C K-edge (285 eV) using a mid-IR driving field. <sup>13,61</sup> Recent studies show that the N and O K-edges (410 and 535 eV) are now also accessible, <sup>30,62-64</sup> indicating that ultrafast spectroscopy of solvated systems in the water window is a frontier, which is now on the horizon. <sup>65,66</sup> XUV and soft x-ray experiments at these higher photon energy will enable in situ measurements of catalytic reaction dynamics with unprecedented time resolution.

Ongoing technological advances are also underway to increase the brightness of these tabletop light sources. The National eXtreme Ultrafast Science Facilty (NeXUS) is one such effort. At the heart of NeXUS is a kW-class ultrafast laser, which will provide a two order of magnitude increase in the XUV pulse repetition rate compared to traditional HHG sources. Similar efforts are also underway through the Extreme Light Infrastructure Attosecond Light Pulse Source (ELI-ALPS). Together these facilities will open the door to a variety of non-linear XUV measurements as well as ultrafast in situ measurements that are currently limited by a lack of sufficient XUV photon flux.

Recent efforts on non-linear experiments using a transient grating approach as well as four wave-mixing experiments show the promise of multidimensional XUV spectroscopy with attosecond time resolution. 67,68 While making phasestable pulses in this domain is challenging, ongoing development of XUV and x-ray optics, interfered-pulse stabilization, and high brilliance tabletop XUV sources with high repetition rates will advance multidimensional spectroscopy to these high energy spectral domains with a extremely high temporal resolution. <sup>69,70</sup> Rapid advances in this developing field promise to provide new physical insights into ultrafast nonadiabatic transitions at conical intersections, where electronic states are degenerate, electrons and nuclei evolve on comparable timescales and thus become strongly coupled. These studies, which are recently accessible in molecular systems, <sup>71</sup> are in the process of being extended to solid surfaces and interfaces in order to provide a molecular understanding of photo-induced electron and nuclear dynamics in relevant material systems. To conclude, XUV spectroscopy of surfaces is an emerging frontier of ultrafast science, and this rapidly growing field is providing needed physical insights required to inform important applications in fields ranging from energy conversion and catalysis to ultrafast spin-based information storage and processing.

## AUTHOR INFORMATION

#### Corresponding Author

Somnath Biswas-Department of Chemistry, Princeton University, Washington Road, Princeton, NJ 08544 Email: somnathb@princeton.edu

**L. Robert Baker**-Department of Chemistry and Biochemistry, The Ohio State University, Columbus, OH 43210 Email: baker.2364@osu.edu

#### Notes

The authors declare no competing financial interest.

### **Biographies**

Somnath Biswas: Somnath Biswas received his BS from Ramakrishna Mission Vidyamandira (Belur, India) in 2013. He obtained his MS from Indian Institute of Technology (Kanpur, India) in 2015. He received his Ph.D. from The Ohio State University under the supervision of Professor L. Robert Baker in 2020. Currently, he is a post-doctoral researcher at Princeton University with Professor Gregory D. Scholes. His research interests are in ultrafast spectroscopy, electron-phonon interaction, surface electronic structure, and quantum information science. He is a recipient of the Presidential Fellowship award from The Ohio State University and the Academic Excellence in Research award from the Federation of Indian Associations, USA.

L. Robert Baker: L. Robert Baker received his BS degree from Brigham Young University in 2007 and his Ph.D. from the University of California, Berkeley, under the supervision of Gabor Somorjai in 2012. Following his Ph.D., he performed postdoctoral research with Stephen Leone before joining The Ohio State University in 2014. His research interests are in ultrafast spectroscopy, heterogeneous catalysis, and surface science. His awards include the Camille Dreyfus Teacher-Scholar Award, AFOSR Young Investigator Award, DOE Early Career Award, Young Innovator Award in NanoEnergy, and The Journal of Physical Chemistry/PHYS Division Lectureship. He serves as principal investigator of the NSF National eXtreme Ultrafast Science (NeXUS) facility.

Acknowledgement Measurements of surface polaron formation in hematite were supported by the Air Force Office of Scientific Research under AFOSR award number FA95550-19-1-0184. Measurements of charge separation on photophysics in CuFeO<sub>2</sub> were supported by the Air Force Office of Scientific Research Young Investigator Award to L.R.B. under AFOSR award number FA9550-15-1-0204. Carrier specific measurements of charge transfer excitons and measurements of ultrafast spin crossover in CoFe<sub>2</sub>O<sub>4</sub> were supported by the Department of Energy Early Career Award to L.R.B. under DOE award number DE-SC0014051. Implementation of the NSF NeXUS facility is supported by the National Science Foundation under NSF award number 1935885. S.B. also thanks the Ohio State Presidential Fellowship Program for support. Sample preparation and characterization was performed at 1) Nanotech West, 2) Nanosystems Lab, 3) Center for Electron Microscopy and Analysis (CEMAS), and 4) Surface Analysis Laboratory each at Ohio State University. We also thank the OSU Chemistry and Biochemistry machine shop for work on the design and construction of the XUV spectrometer.

## References

- Biswas, S.; Husek, J.; Londo, S.; Baker, L. R. Highly Localized Charge Transfer Excitons in Metal Oxide Semiconductors. *Nano Lett.* 2018, 18, 1228–1233.
- (2) Biswas, S.; Wallentine, S.; Bandaranayake, S.; Baker, L. R. Controlling polaron formation at hematite surfaces by molecular functionalization probed by XUV reflection-absorption spectroscopy. J. Chem. Phys. 2019, 151, 104701.
- Husek, J.; Cirri, A.; Biswas, S.; Asthagiri, A.; Baker, L. R. Hole Thermalization Dynamics Facilitate Ultrafast Spatial Charge Separation in CuFeO2 Solar Photocathodes. J. Phys. Chem. C 2018, 122, 11300-11304, DOI: 10.1021/acs.jpcc.8b0296.
   Lorde S.; Pigrage S.; Husel, L.; Pinchell, L. W. New.
- (4) Londo, S.; Biswas, S.; Husek, J.; Pinchuk, I. V.; New-burger, M. J.; Boyadzhiev, A.; Trout, A. H.; McComb, D. W.;

- Kawakami, R.; Baker, L. R. Ultrafast Spin Crossover in a Room-Temperature Ferrimagnet: Element-Specific Spin Dynamics in Photoexcited Cobalt Ferrite. *J. Phys. Chem. C* **2020**, *124*, 11368–11375.
- (5) Nguyen, L.; Tao, F. F.; Tang, Y.; Dou, J.; Bao, X.-J. Understanding catalyst surfaces during catalysis through near ambient pressure X-ray photoelectron spectroscopy. *Chem. Rev.* 2019, 119, 6822–6905.
- (6) Somorjai, G. A.; Li, Y. Impact of surface chemistry. Proc. Natl. Acad. Sci. 2011, 108, 917.
- (7) Marsh, B. M.; Vaida, M. E.; Cushing, S. K.; Lamoureux, B. R.; Leone, S. R. Measuring the surface photovoltage of a Schottky barrier under intense light conditions: Zn/p-Si(100) by laser time-resolved extreme ultraviolet photoelectron spectroscopy. J. Phys. Chem. C 2017, 121, 21904-21912, DOI: 10.1021/acs.jpcc.7b06406.
- (8) Nilsson, A.; Pettersson, L. G.; Norskov, J. Chemical bonding at surfaces and interfaces: Elsevier, 2011.
- surfaces and interfaces; Elsevier, 2011.
   Muiño, R. D.; Sánchez-Portal, D.; Silkin, V. M.; Chulkov, E. V.; Echenique, P. M. Time-dependent electron phenomena at surfaces. Proc. Natl. Acad. Sci. U.S.A. 2011, 108, 971-976.
- (10) Stähler, J.; Bovensiepen, U.; Meyer, M.; Wolf, M. A surface science approach to ultrafast electron transfer and solvation dynamics at interfaces. Chem. Soc. Rev. 2008, 37, 2180-2190
- namics at interfaces. Chem. Soc. Rev. 2008, 37, 2180–2190.

  (11) Folorunso, A. S.; Bruner, A.; Mauger, F.; Hamer, K. A.; Hernandez, S.; Jones, R. R.; DiMauro, L. F.; Gaarde, M. B.; Schafer, K. J.; Lopata, K. Molecular Modes of Attosecond Charge Migration. Phys. Rev. Lett. 2021, 126, 133002.
- (12) Calegari, F.; Trabattoni, A.; Palacios, A.; Ayuso, D.; Castro-villi, M. C.; Greenwood, J. B.; Decleva, P.; Martín, F.; Nisoli, M. Charge migration induced by attosecond pulses in bio-relevant molecules. *Journal of Physics B: Atomic, Molecular and Optical Physics* 2016, 49, 142001.
- (13) Attar, A. R.; Bhattacherjee, A.; Pemmaraju, C. D.; Schnorr, K.; Closser, K. D.; Prendergast, D.; Leone, S. R. Femtosecond x-ray spectroscopy of an electrocyclic ring-opening reaction. *Science* 2017, 356, 54-59, DOI: 10.1126/science.aaj2198.
- (14) Kobayashi, Y.; Chang, K. F.; Zeng, T.; Neumark, D. M.; Leone, S. R. Direct mapping of curve-crossing dynamics in IBr by attosecond transient absorption spectroscopy. *Science* 2019, 365, 79–83.
- (15) Zhang, K.; Ash, R.; Girolami, G. S.; Vura-Weis, J. Tracking the Metal-Centered Triplet in Photoinduced Spin Crossover of Fe (phen) 32+ with Tabletop Femtosecond M-Edge X-ray Absorption Near-Edge Structure Spectroscopy. Journal of the American Chemical Society 2019, 141, 17180-17188.
- can Chemical Society 2019, 141, 17180-17188.

  (16) Li, J.; Lu, J.; Chew, A.; Han, S.; Li, J.; Wu, Y.; Wang, H.; Ghimire, S.; Chang, Z. Attosecond science based on high harmonic generation from gases and solids. Nat. Commun. 2020, 11, 1-13
- (17) de Groot, F. M. F. Multiplet Effect in X-ray Spectroscopy. Coord. Chem. Rev. 2005, 249, 31-63
- ord. Chem. Rev. 2005, 249, 31-63.

  (18) Vura-Weis, J.; Jiang, C.-M.; Liu, C.; Gao, H.; Lucas, J. M.; de Groot, F. M. F.; Yang, P.; Alivisatos, A. P.; Leone, S. R. Femtosecond M<sub>2,3</sub> = Edge Spectroscopy of Transition-Metal Oxides: Photoinduced Oxidation State Change in α-Fe<sub>2</sub>O<sub>3</sub>. J. Phys. Chem. Lett. 2013, 4, 3667–3671, DOI: 10.1021/jz401997d.
- (19) Cushing, S. K.; Porter, I. J.; de Roulet, B. R.; Lee, A.; Marsh, B. M.; Szoke, S.; Vaida, M. E.; Leone, S. R. Layerresolved ultrafast extreme ultraviolet measurement of hole transport in a Ni-TiO2-Si photoanode. Sci. Adv 2020, 6, eaav6650
- (20) de Groot, F. High-resolution X-ray emission and X-ray absorption spectroscopy. Chem. Rev. 2001, 101, 1779–1808, DOI: 10.1021/cr9900681.
- (21) Bressler, C.; Chergui, M. Ultrafast X-ray Absorption Spectroscopy. *Chem.Rev.* **2004**, *104*, 1781–1812, DOI: 10.1021/cr0206667.
- (22) Zhang, K.; Lin, M.-F.; Ryland, E. S.; Verkamp, M. A.; Benke, K.; De Groot, F. M.; Girolami, G. S.; Vura-Weis, J. Shrinking the synchrotron: Tabletop extreme ultraviolet absorption of transition-metal complexes. J. Phys. Chem. Lett. 2016, 7, 3383-3387.
- (23) Lin, M.-F.; Verkamp, M. A.; Leveillee, J.; Ryland, E. S.; Benke, K.; Zhang, K.; Weninger, C.; Shen, X.; Li, R.; Fritz, D.; Bergmann, U.; Wang, X.; Schleife, A.; Vura-Weis, J. Carrier-Specific Femtosecond XUV Transient Absorption of PbI2 Reveals Ultrafast Nonradiative Recombination. J. Phys. Chem. C 2017, 121, 27886-27893, DOI: 10.1021/acs.jpcc.7b11147.
- (24) Hayes, D.; Hadt, R. G.; Emery, J. D.; Cordones, A. A.; Martinson, A. B.; Shelby, M. L.; Fransted, K. A.; Dahlberg, P. D.; Hong, J.; Zhang, X.; Chen, L. Electronic and nuclear contributions to time-resolved optical and X-ray absorption spectra of hematite and insights into photoelectrochemical performance. Energy Environ. Sci. 2016, 9, 3754-3769.
- hematite and insights into photoelectrochemical performance.

  Energy Environ. Sci. 2016, 9, 3754–3769.

  (25) Cirri, A.; Husek, J.; Biswas, S.; Baker, L. R. Achieving Surface Sensitivity in Ultrafast XUV Spectroscopy: M2, 3-Edge Reflection—Absorption of Transition Metal Oxides. J. Phys. Chem. C 2017, 121, 15861–15869.
- (26) Biswas, S.; Husek, J.; Baker, L. R. Elucidating ultrafast electron dynamics at surfaces using extreme ultraviolet (XUV) reflection—absorption spectroscopy. Chem. Commun. 2018, 54, 4216–4230.
- (27) Husek, J.; Cirri, A.; Biswas, S.; Baker, L. R. Surface electron dy-

- namics in hematite ( $\alpha$ -Fe 2 O 3): correlation between ultrafast surface electron trapping and small polaron formation. Chem. Sci. 2017, 8, 8170-8178.
- Londo, S.; Biswas, S.; Pinchuk, I. V.; Boyadzhiev, A.; Kawakami, R.; Baker, L. R. Ultrafast Optical Spin Switch Pinchuk, I. V.; Boyadzhiev, A.; ing in Ferrimagnetic Nickel Ferrite (NiFe $_2$ O $_4$ ) Studied by XUV Reflection-Absorption Spectroscopy. J. Phys. Chem. C **2022**, DOI: 10.1021/acs.jpcc.1c09763.
- Bandaranayake, S.; Hruska, E.; Londo, S.; Biswas, S.; Baker, L. R. Small Polarons and Surface Defects in Metal Oxide Photocatalysts Studied Using XUV Reflection—Absorption Spectroscopy. J. Phys. Chem. C 2020, 124, 22853—22870. Johnson, A. S.; Wood, D.; Austin, D. R.; Brahms, C.; Gregory, A.; Holzner, K. B.; Jarosch, S.; Larsen, E. W.; Parker, S.; Strüber, C.; Ye, P.; John, W. G. T.; Marangos, J. P. Appara-
- tus for soft x-ray table-top high harmonic generation. Rev. Sci. Instrum 2018, 89, 083110.
- (31) Liu, L.; Mei, Z.; Tang, A.; Azarov, A.; Kuznetsov, A.; Xue, Q.-K.; Du, X. Oxygen vacancies: The origin of *n*-type conductivity in ZnO. *Phys. Rev. B* **2016**, *93*, 235305. Bjorheim, T. S.; Arrigoni, M.; Saeed, S. W.; Kotomin, E.;
- Maier, J. Surface Segregation Entropy of Protons and Oxygen Vacancies in BaZrO3. Chem. Mater. 2016, 28, 1363–1368, DOI: 10.1021/acs.chemmater.5b04327.
- (33) Fernandez-Serra, M.; Adessi, C.; Blase, X. Surface segregation and backscattering in doped silicon nanowires. Phys. Rev. Lett. **2006**, 96, 166805.
- Arias, T.; Joannopoulos, J. Electron trapping and impurity segregation without defects: Ab initio study of perfectly rebonded grain boundaries. *Phys. Rev. B.* **1994**, *49*, 4525. Goodvin, G. L.; Covaci, L.; Berciu, M. Holstein polarons near surfaces. *Phys. Rev. Lett.* **2009**, *103*, 176402.
- Di Valentin, C.; Selloni, A. Bulk and Surface Polarons in Photoexcited Anatase TiO2. J. Phys. Chem. Lett. 2011, 2, 2223-
- 2228, DOI: 10.1021/jz2009874.

  Nourafkan, R.; Capone, M.; Nafari, N. Surface polaron formation in the Holstein model. *Phys. Rev. B* **2009**, *80*, 155130.

  Henke, B. L.; Gullikson, E. M.; Davis, J. C. X-ray Interactions: Photoabsorption, Scattering, Transmission, and Reflection at E= 50-30,000 eV, Z= 1-92. *At. Data Nucl. Data Tables* **1993**, 57, 181, 242 *54*, 181–342.
- (39) Kaplan, C. J.; Kraus, P. M.; Gullikson, E. M.; Borja, L.; Cushing, S. K.; Zürch, M.; Chang, H.-T.; Neumark, D. M.; Leone, S. R. Retrieval of the complex-valued refractive index of germanium near the M 4, 5 absorption edge. JOSA B 2019, *36*, 1716–1720.
- Chen, W.; Xiong, W. Polaron-formation revealed by transient XUV imaginary refractive index changes in different iron compounds. *Phys. Chem. Chem. Phys.* **2021**, *23*, 4486–4490.

  Jiang, C.-M.; Baker, L. R.; Lucas, J. M.; Vura-Weis, J.; Alivisatos, A. P.; Leone, S. R. Characterization of Photo-
- Induced Charge Transfer and Hot Carrier Relaxation Pathways in Spinel Cobalt Oxide (Co3O4). J. Phys. Chem. C 2014, 118, 22774–22784, DOI: 10.1021/jp5071133.

  Carneiro, L. M.; Cushing, S. K.; Liu, C.; Su, Y.; Yang, P.; Alivisatos, A. P.; Leone, S. R. Excitation-wavelength-dependent
- small polaron trapping of photoexcited carriers in  $\alpha$ -Fe 2 O 3.
- Nat. Mater 2017, 16, 819.
  (43) Pastor, E.; Park, J.-S.; Steier, L.; Kim, S.; Grätzel, M.; Durrant, J. R.; Walsh, A.; Bakulin, A. A. In situ observation of picosecond polaron self-localisation in α-Fe 2 O 3 photoelectrochemical cells. Nat. Commun. 2019, 10, 1–7.
- (44) Porter, I. J.; Cushing, S. K.; Carneiro, L. M.; Lee, A.; Ondry, J. C.; Dahl, J. C.; Chang, H.-T.; Alivisatos, A. P.; Leone, S. R. Photoexcited small polaron formation in goethite ( $\alpha$ -FeOOH) nanorods probed by transient extreme ultraviolet spectroscopy. J. Phys. Chem. Lett. **2018**, 9, 4120–4124.
- Kerisit, S.; Rosso, K. M. Computer simulation of electron transfer at hematite surfaces. Geochim. Cosmochim. Acta 2006, 70, 1888-1903.
- Iordanova, N.; Dupuis, M.; Rosso, K. M. Charge transport in metal oxides: a theoretical study of hematite  $\alpha$ -Fe<sub>2</sub>O<sub>3</sub>. *J. Chem. Phys.* **2005**, *122*, 144305.
- Deskins, N. A.; Dupuis, M. Electron transport via polaron hopping in bulk Ti O 2: A density functional theory characteriza-
- Ton. Phys. Rev. B 2007, 75, 195212.

  Zurch, M.; Chang, H.-T.; Borja, L. J.; Kraus, P. M.; Cushing, S. K.; Gandman, A.; Kaplan, C. J.; Oh, M. H.; Prell, J. S.; Prendergast, D.; Pemmaraju, C. D.; Neumark, D. M.; Leone, S. R. Direct and simultaneous observation of ultrafast electron and hole dynamics in germanium. Nat. Commun. **2017**, 8, 15734.
- (49) Pace, G.; Bargigia, I.; Noh, Y.-Y.; Silva, C.; Caironi, M. Intrinsically distinct hole and electron transport in conjugated polymers controlled by intra and intermolecular interactions. Nat. Commun. 2019, 10, 1-11.
- Cannelli, O.; Colonna, N.; Puppin, M.; Rossi, T. C.; Kinschel, D.; Leroy, L. M.; Löffler, J.; Budarz, J. M.; March, A. M.; Doumy, G.; Al Haddad, A.; Tu, M. F.; Kumagai, Y.; Walko, D.; Smolentsev, G.; Krieg, F.; Boehme, S. C.; Kovalenko, M. V.; Chergui, M.; Mancini, G. F. Quantifying Photoinduced Polaronic Distortions in Inorganic Lead Halide Perovskite Nanocrystals. J. Am. Chem. Soc. 2021, 143, 9048–9059, DOI 10.1021/JACS.1C02403/SUPPL\_FILE/JA1C02403\_SI\_001.PDF.

- (51) Santomauro, F. G.; Grilj, J.; Mewes, L.; Nedelcu, G.; Yakunin, S.; Rossi, T.; Capano, G.; Al Haddad, A.; Budarz, J.; Kinschel, D.; Ferreira, D. S.; Rossi, G.; Gutierrez Tovar, M.; Grolimund, D.; Samson, V.; Nachtegaal, M.; Smolentsev, G.; Kovalenko, M. V.; Chergui, M. Localized holes and delocalized electrons in photoexcited inorganic perovskites: Watching each atomic actor by picosecond X-ray absorption spectroscopy. Struct. Dyn 2017, 4, 044002, DOI: 10.1063/1.4971999.
- Penfold, T. J.; Szlachetko, J.; Santomauro, F. G.; Britz, A.; Gawelda, W.; Doumy, G.; March, A. M.; Southworth, S. H.; Rittmann, J.; Abela, R.; Chergui, M.; Milne, C. J. Revealing
- hole trapping in zinc oxide nanoparticles by time-resolved X-ray spectroscopy. *Nat. Commun.* **2018**, *9*, 1–9. de Groot, F. M. F.; Grioni, M.; Fuggle, J. C.; Ghijsen, J.; Sawatzky, G. A.; Petersen, H. Oxygen 1s x-ray-absorption edges of transition-metal oxides. Phys. Rev. B 1989, 40, 5715-5723, DOI: 10.1103/PhysRevB.40.5715.
- (54) Cushing, S. K.; Zürch, M.; Kraus, P. M.; Carneiro, L. M.; Lee, A.; Chang, H.-T.; Kaplan, C. J.; Leone, S. R. Hot phonon and carrier relaxation in Si (100) determined by transient ex-
- treme ultraviolet spectroscopy. Struct. Dyn 2018, 5, 054302.
  (55) Kaplan, C. J.; Kraus, P. M.; Ross, A. D.; Zürch, M.; Cushing, S. K.; Jager, M. F.; Chang, H.-T.; Gullikson, E. M.; Neumark, D. M.; Leone, S. R. Femtosecond tracking of carrier relaxation in germanium with extreme ultraviolet transient reflectivity. Phys. Rev. B 2018, 97, 205202.
- (56) Zurch, M.; Chang, H.-T.; Kraus, P. M.; Cushing, S. K.; Borja, L. J.; Gandman, A.; Kaplan, C. J.; Oh, M. H.; Prell, J. S.; Prendergast, D.; Pemmaraju, C. D.; Neumark, D. M.; Leone, S. R. Ultrafast carrier thermalization and trapping in silicon-germanium alloy probed by extreme ultraviolet transient absorption spectroscopy. Struct. Dyn. 2017, 4, 044029, DOI: 10.1063/1.4985056.
- Attar, A. R.; Chang, H.-T.; Britz, A.; Zhang, X.; Lin, M.-F.; Krishnamoorthy, A.; Linker, T.; Fritz, D.; Neumark, D. M.; Kalia, R. K.; Nakano, A.; Ajayan, P.; Vashishta, P.; Bergmann, U.; Leone, S. R. Simultaneous observation of carrierspecific redistribution and coherent lattice dynamics in 2H-MoTe2 with femtosecond core-level spectroscopy. ACS nano **2020**, *14*, 15829–15840.
- (58) Yang, X.; Fugate, E. A.; Mueanngern, Y.; Baker, L. R. Photoelectrochemical CO<sub>2</sub> Reduction to Acetate on Iron-Copper Oxide Catalysts. ACS Catal. 2016, 7, 177-180.
  (59) Fugate, E. A.; Biswas, S.; Clement, M. C.; Kim, M.; Kim, D.;
- Asthagiri, A.; Baker, L. R. The role of phase impurities and lattice defects on the electron dynamics and photochemistry of CuFeO 2 solar photocathodes. *Nano Res.* **2019**, *12*, 2390–2399. Jiang, C.-M.; Reyes-Lillo, S. E.; Liang, Y.; Liu, Y.-S.; Liu, G.; Toma, F. M.; Prendergast, D.; Sharp, I. D.; Cooper, J. K. Elec-
- tronic structure and performance bottlenecks of CuFeO2 photocathodes. Chem. Mater. 2019, 31, 2524-2534.
- (61) Popmintchev, T.; Chen, M.-C.; Popmintchev, D.; Arpin, P.; Brown, S.; Ališauskas, S.; Andriukaitis, G.; Balčiunas, T.; Mücke, O. D.; Pugzlys, A.; Baltuška, A.; Shim, B.; Schrauth, S. E.; Gaeta, A.; Hernández-García, C.; Plaja, L.; Becker, A.; Jaron-Becker, A.; Murnane, M. M.; Kapteyn, H. C. Bright coherent ultrahigh harmonics in the keV x-ray regime from mid-infrared femtosecond lasers. Science 2012, 336, 1287-
- Silva, F.; Teichmann, S. M.; Cousin, S. L.; Hemmer, M.; Biegert, J. Spatiotemporal isolation of attosecond soft X-ray pulses in the water window. Nat. Commun. 2015, 6, 1-6.
- Timoshenko, J.; Roldan Cuenya, B. In situ/operando electrocatalyst characterization by X-ray absorption spectroscopy. Chem. Rev. **2020**, 121, 882–961.
- (64) Pertot, Y.; Schmidt, C.; Matthews, M.; Chauvet, A.; Huppert, M.; Svoboda, V.; Von Conta, A.; Tehlar, A.; Baykusheva, D.; Wolf, J.-P.; Wörner, H. J. Time-resolved x-ray absorption spectroscopy with a water window high-harmonic source. Science 2017, 355, 264–267.
- (65) Kleine, C.; Ekimova, M.; Goldsztejn, G.; Raabe, S.; Struber, C.; Ludwig, J.; Yarlagadda, S.; Eisebitt, S.; Vrakking, M. J.; Elsaesser, T.; Nibbering, E. T. J.; Rouzée, A. Soft X-ray absorption spectroscopy of aqueous solutions using a table-top femto second soft X-ray source. J. Phys. Chem. Lett. 2018, 10,
- (66) Smith, A. D.; Balciunas, T.; Chang, Y.-P.; Schmidt, C.; Zinchenko, K.; Nunes, F. B.; Rossi, E.; Svoboda, V.; Yin, Z.; Wolf, J.-P.; Wörner, H. J. Femtosecond soft-x-ray absorption spectroscopy of liquids with a water-window high-harmonic Source. J. Phys. Chem. Lett. 2020, 11, 1981–1988.
- (67) Marroux, H. J.; Fidler, A. P.; Neumark, D. M.; Leone, S. R. Multidimensional spectroscopy with attosecond extreme ultraviolet
- and shaped near-infrared pulses. Sci. Adv 2018, 4, eaau3783.
  Cao, W.; Warrick, E. R.; Fidler, A.; Leone, S. R.; Neumark, D. M. Near-resonant four-wave mixing of attosecond extreme-ultraviolet pulses with near-infrared pulses in neon: Detection of electronic coherences. Phys. Rev. A 2016, 94, 021802.
- Tross, J.; Kolliopoulos, G.; Trallero-Herrero, C. A. Self referencing attosecond interferometer with zeptosecond precision. Optics express 2019, 27, 22960–22969.
- Wituschek, A.; Kornilov, O.; Witting, T.; Maikowski, L.; Stienkemeier, F.; Vrakking, M. J.; Bruder, L. Phase cycling of

- extreme ultraviolet pulse sequences generated in rare gases. New J. Phys 2020, 22, 092001.

  (71) Neville, S. P.; Chergui, M.; Stolow, A.; Schuurman, M. S. Ultrafast x-ray spectroscopy of conical intersections. Phys. Rev. Lett. 2018, 120, 243001.

## For Table of Contents Only

